Method Comparisons for Wake Model and Optimization Algorithm Selection in Wind Farm Layout Optimization

Nicholas F. Baker*, Andrew P. J. Stanley†, and Andrew Ning‡
Brigham Young University, Provo, Utah 84602.

Katherine Dykes§
Danmarks Tekniske Universitet, 2800 Kgs. Lyngby, Denmark.

I. Introduction

Optimization problems regarding in the layout of wind farms draw upon multivariate input and produce multimodal output. Analyzing selections of the many possible inputs (turbine cost, turbine location, wind data granularity, geographic peculiarities, etc.) and many possible target function outputs (minimized construction costs, maximize energy production, minimized environmental impact, etc.) can make these problems as simplistic or complicated as the user desires. Computer automated modelling assists in analyzing variable permutations and optimizing target function calculations on a scale far greater than could be accomplished solely through real-world experimentation. Yet for these computer optimizations to be successful, two separate factors must be addressed:

1) Choice of model inputs/outputs
2) Optimization algorithm selection

Sub-optimal turbine placement results in lost energy and potentially millions of forfeit dollars over the course of a wind farm's typical 20-year life-span [1]. Such errors could result from inaccurate wake models or inefficient optimization algorithms. Mistakes in either of these two areas could be avoided with a clearer understanding of model and optimization best practices.

The rotating blades of a horizontal wind turbine sweep out a circular geometry, and create a wake [2]. This wake both slows the free stream air passing through its face, and increases the diameter of the affected wind volume. This three-dimensional wake volume is characterized by both a wind velocity decrease and a turbulence increase [3]. As a result, downstream rotors in the wake-affected area experience reduced power production (due to the decreased wind velocity) and a shortened lifespan (as a result of the increased turbulence intensity) [4]. Since waked turbines result in both decreased energy production and reduced turbine lifespan, wakes become an important consideration in windfarm design [1].

Wake and turbulence modeling have been described as "two of the most challenging research topics in the field of fluid mechanics and are considered unsolved problems in classic physics" [1]. The two general approaches taken to solve these complicated issues are (1) computationally inexpensive, simplified theoretical wake models, formulated to correlate to empirical data from the waked region [4–6], or (2) computationally expensive approaches, using the Reynolds-Averaged Navier-Stokes (RANS) equations, Large-Eddy Simulations (LES), or Direct Numerical Simulation (DNS), which far better increase the accuracy and granularity of their results[7]. Many engineering wake models (EWMs) have been created, varying both their complexity and approach to the problem. While some account for 2-D and 3-D phenomena, the simplest and most widely used wake model was created by Jensen [8] and is 1-Dimensional. A more complicated EWM which takes into account all 3 dimensions was created by Bastankhah, and uses Gaussian curves for continuous and differentiable wake calculations.

Optimization through iteration using models based on the RANS equations take on the scale of several hours to converge to a solution. More complex still, LES models can take up to several weeks until convergence. And finally, a DNS analysis, at least at the time attempted by Soren et. al in 2011 [7], was infeasible in terms of computational time. However, once an optimized solution has been reached by one of the simpler models described previously, a single LES can be run to validate the proposed optimized wind farm layout.

*Masters Student, Department of Mechanical Engineering, 360 EB, Provo, UT 84602, AIAA Student Member
†Ph.D. Candidate, Department of Mechanical Engineering, 360 EB, Provo, UT 84602, AIAA Student Member
‡Assistant Professor, Department of Mechanical Engineering, 360 EB, Provo, UT 84602, AIAA Senior Member
§DTU

Optimization refers to algorithms that conduct incremental calculations on input variables in an attempt to maximize or minimize some output target function or functions. Optimization algorithms can be broadly categorized as either (1) gradient-based, or (2) gradient-free. Gradient based algorithms require that the governing functions be continuous, differentiable, and that derivatives can be calculated. They scale well to large problems and are efficient at finding local optimums, but have difficulties with functions that are “noisy" or when discontinuities are present [9]. Gradient free algorithms can be used if derivatives can’t be obtained, but are usually much slower than gradient-based algorithms and don’t always scale well. Gradient-free algorithms are able to escape local optimums and are generally easier to implement. Both types can be used if the objective function isn’t known, but gradient-based algorithms greatly reduce computational time if it both knows the objective function and can calculate the derivatives [10].

Many papers have been written on various EWMs, and even more have been written on optimizations algorithms. However little has been published on comparative pairings of the two in the area of wind farm technology, and how they play out with wind farm characteristics (i.e. geography, wind resource, etc.) An internationally collaborative study was conducted by the International Energy Association (IEA) for modelling and optimizing blade geometry [11] in 2017, but our research indicates that our case studies are the first time such a study has been conducted to comparatively and empirically analyze optimization methods and EWM selection on a broad wind farm layout optimization problem.

We therefore undertook designing a series of simplified wind farm scenarios formed into case studies, where participants would choose model and method pairings to discover as optimal a solution as they were able. Our intent is to assist researchers in the field by presenting a standardized method of comparing widn farm layout optimization methods. Case studies 1 and 2 (cs1 & cs2) were wind farm scenarios with circular boundaries of three differnt sizes to observe patterns over increasing complexity. Case studies 3 and 4 (cs3 & cs4) introduced both non-uniform boundaries and a more complicated wind resource than cs1 & cs2, to further test participant methods.

Mention cs3 & cs4 results here

II. Methodology

Feedback we received from particiants of cs1 & cs2 were that those wind farm scenarios were too simplistic. The simplicity was by design, to both incentivize participation and to permit the case study results to have general application. But with that feedback in mind, for cs3 & cs4 we chose to increase the complexity of both the wind resource and the wind farm boundary.

Regarding the wind farm boundary, one cs1 participant requested we use a geography that existed in the real world, as opposed to the contrived ones used in the first two studies. We therefore selected for our model parcels III and IV of the Borssele Wind Farm (depicted in Fig. 1), which is located in the North Sea between the Netherlands and England. This farm offered two characteristics that gradient-based optimizers would have difficulty with: (1) concavities in the boundaries (2) disjoint boundary sections. The boundary sizing was scaled so that the model turbines we used could be adequately spaced (depicted in Fig. 2), but the boundary contours are those of the real-world farm.

The first two case studies gave a simplified wind resource of sixteen (16) discrete bins and a constant wind speed across all directions. To increase realism in cs3 & cs4 we gave participants twenty (20) discrete directional bins, with twenty (20) wind speed probabilities at each bin, giving four-hundered (400) pieces of wind information in cs3 & cs4 as opposed to the sixteen (16) given in cs1 & cs2.

For cs3 the goal was to isolate variability in participants’ optimization methods. In order to do this we pre-coded a representative wake model as a control variable and permitted participants to use any optimization strategy they desire to alter turbine locations that would deliver the best annual energy production (AEP) for the farm. We used only parcel IIIa of the Borssele farm in cs3, since it includes concavities but avoids the disjoint boundary problem.

The cs4 boundary invloved five parcels from the Borssele farm. Besides adding the complexity of disjoint boundary sections, we also permitted participants to use whatever wake model they chose for optimization purposes, though final comparisons would be conducted with our supplied model. The wake model we supplied was used in cs1, and is a modification of Bastankhah’s Gaussian wake model. The continuity of this wake model’s output permits use of both gadient and non-gradient based optimization methods.

A. Common to Both Case Studies

Though testing for different variables, certain charactersistics were common to both cs3 & cs4. A brief list of these common variables is described in the following section.

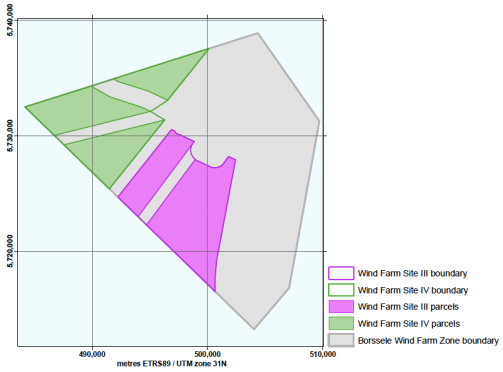

Figure 1 Borssele farm outline as presented in the NEA's document calling for bids.[12]

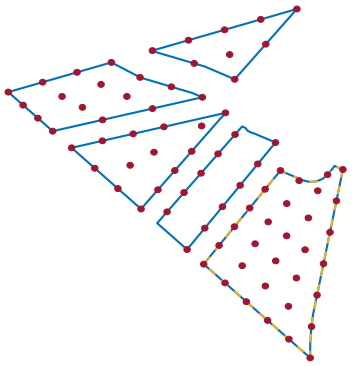

Figure 2 Graphical depiction of the boundaries and example layout we used for cs3 and cs4. The only boundary segment used in cs3 is in the bottom right, denoted by a dashed yellow and blue boundary.

1. Wind Turbine Specifications

We used the IEA 10 MW offshore reference turbine[13] in cs3 & cs4, since the wind farm scenarios are modelled after an offshore location. This turbine's attributes are open source, and the turbine is designed as baseline for offshore wind turbine specifications. The power curve for the IEA 10 MW turbine is defined as shown in Eq. (1) and Fig. 3. The turbine specifications necessary for our simplified version of Bastankhah's Gaussian wake model used in cs3 are shown in Table 1.

$$P(V) = \begin{cases} 0 & V < V_{cut\text{-}in} \\ P_{rated}\left(\frac{V - V_{cut\text{-}in}}{V_{rated} - V_{cut\text{-}in}}\right)^3 & V_{cut\text{-}in} \leq V < V_{rated} \\ P_{rated} & V_{rated} \leq V < V_{cut\text{-}out} \\ 0 & V \geq V_{cut\text{-}out} \end{cases} \tag{1}$$

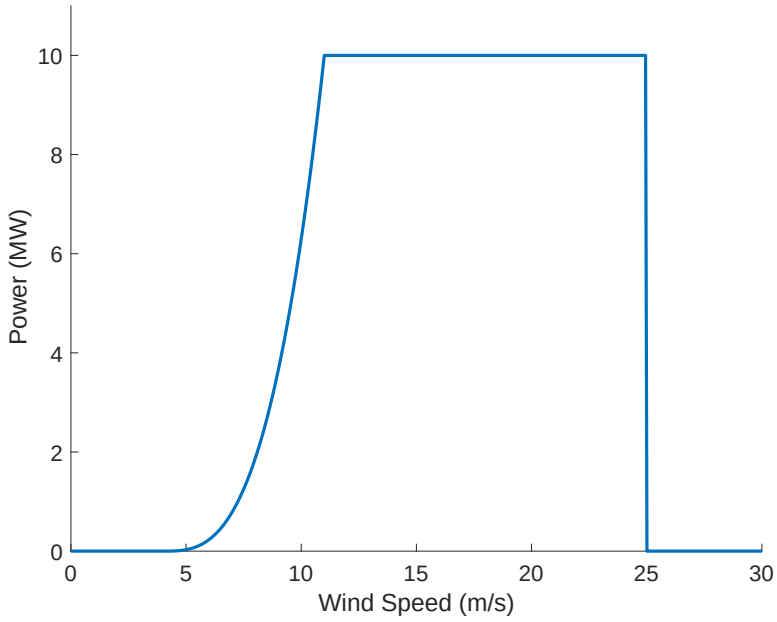

Figure 3 Graphical depiction of IEA's 10-MW onshore reference turbine's power curve.

Table 1 Attributes for IEA's 10-MW onshore reference turbine

Rotor Diameter	198	m
Turbine Rating	10	MW
Cut-In Wind Speed	4	m/s
Rated Wind Speed	11	m/s
Cut-Out Wind Speed	25	m/s

2. Farm Geography

To focus on optimization method and EWM variability, as well as to avoid introducing too many unnecessary variables, the wind farms for all scenarios were on flat and calm seas. Our version of the Borssele farm geography was adapted from coordinates supplied by an open solicitation for bids announced in August of 2016 by the Netherlands Enterprise Agency (NEA)[12]. There are neighboring farm sections already built (in the grayed out area in figure Fig. 1), but for our purposes we only utilize portions III and IV, disregarding neighboring allottments to reduce complexity.

Top performers from cs1 & cs2 used gradient based optimization methods, and in hindsight the simplicity of farm geography in those case studies may have favored such methods. The selection of the Borssele geography was in part to give difficulty to the successful methods from cs1 & cs2, through both concavities and non-contigous regions.

For cs1 & cs2, the number of turbines for each increasing farm diameter were all prime numbers. Sticking with this theme, in cs3 & cs4 we again chose a prime number of turbines. However initial tests demonstrated that, with the 10MW turbine, eighty-one (81) turbines would be too sparse a farm for interesting wake effects. Instead of increasing the number of turbines beyond this (which may have prohibitively increased the computational requirements for some participants), we scaled down the boundary proportions by about half, which gave us a density we felt would deliver interesting optimization results.

As a further alteration, the original Borssele announcement required that turbine radii be contained entirely within the boundary. To accommodate this requirement, yet also give our participant optimizers less math to compute, boundaries were again altered inwardly by the 10MW turbine's radius, meaning that now turbine (x, y) hub locations could be

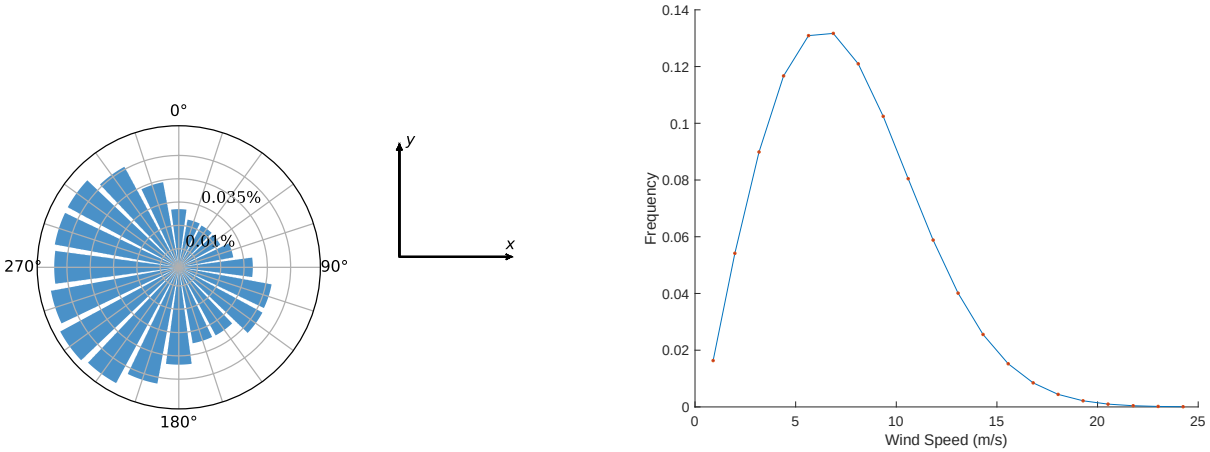

Figure 4 (left) Wind frequency distribution over the 20 bins for the windrose used in cs3 and cs4. (right) Wind speed frequency distribution at one of the wind directions (30°).

anywhere on or whithin the supplied boundary limits. As a final turbine constraint, we further mandated that turbines must be placed no less than two rotor diameters apart from any other turbine.

A single example layout for each case study was supplied (displayed in Fig. 2), meant to give a baseline AEP output for which all participants could optimize beyond. The placement was largely automated to be an evenly spaced grid contoured to the boundaries, but for certain spots giving difficulty (like outcroppings), turbines were placed by hand by the author. This layout only serves as an AEP measure by which participant submissions can be judged so as to determine relative target function improvement. Participants are not required to use these layouts as starting points for their optimizations, though they have the option to do so.

3. Wind Attributes

After completing a convergence study, we found resonable convergence in AEP calculation occured using no more than 20 wind directional bins. This study did not run optimizations from these differing number of bins, it simply analyzed single target function calculations. Had we run optimizations with varying bin numbers, we may have found more bins to have be necessary, but that can be explored in future work.

The frequency distribution for each of our 20 bins is depicted graphically in polar coordinates on the left side of Fig. 4. In this figure, a greater magnitude in the radial direction from the origin indicates a higher wind frequency from that specific direction. Each of the 20 binned directions have a unique frequency distribution that follows a Weibull curve, discretized for 20 values. An example frequency distribution for the direction of 30° is depicted on the right side of Fig. 4.

B. Case Study 3: Non-Convex Boundary

Mirrorring cs1, the purpose of cs3 was to isolate optimization practices for WFLO with boundaries having concavities. To isolate this variable, we mandated that participants use a single representative EWM. We selected a generalized EWM that could be used by both gradient-based and gradient-free optimization algorithms, that was also computationally inexpensive in comparison to LES and DNS methods.

1. Wake Model

The wake model selected for cs3 is the same used in cs1, a simplified version of Bastankhah's Gaussian wake model [14, 15]. This wake model is described Eq. (2).

$$\frac{\Delta U}{U_\infty} = \left(1 - \sqrt{1 - \frac{C_T}{8\sigma_y^2/D^2}}\right)\exp\left(-0.5\left(\frac{y-\delta}{\sigma_y}\right)^2\right) \tag{2}$$

In Eq. (2), $\Delta U/U_\infty$ is the wake velocity deficit, $C_T = 8/9$ is the thrust coefficient, $y - \delta$ is the distance of the point of interest from the wake center in the cross-stream horizontal direction, D is the turbine diameter, and σ_y is the standard deviation of the wake spread in the cross-stream horizontal direction as defined in Eq. (3):

$$\sigma_y = (k_y x) + \frac{D}{\sqrt{8}} \tag{3}$$

In Eq. (3), x is the downstream distance from the turbine generating the wake to the turbine of interest, and D is the turbine diameter. The variable k_y is determined as a function of turbulence intensity (I). In this case study turbulence intensity was treated as a constant of 0.075, and we therefore used a corresponding k_y of 0.0324555 [15, 16].

Increasing turbulence intensity has numerous effects and draws attention away from the main purpose of these case studies, which was to observe the differences of optimization strategies. For the wake model we used (shown in Eq. (2)), increasing the turbulence intensity widened the wake cone, but second and third order effects are unknown. As such, we used a very low intensity in an attempt to minimize the considered variables.

2. Number of Turbines

Though cs1 & cs2 used multiple farm sizes to observe the effects of scaling, the focus of cs3 is to observe methods regarding the unique boundary geography. For this reason, only a single sized farm is used in cs3, consisting of twenty-five (25) turbines. Like cs1 & cs2, the number of turbines for cs3 & cs4 were selected as perfect squares.

3. Supplied Code

We provided participants with a link to a GitHub repository* which included files with the following contents:

- Turbine characteristics, wind frequency, and wind speed in IEA 37's `.yaml` schema
- Boundary coordinates and an example turbine layout (in `.yaml` format)
- Python parsers of the `.yaml` schema
- Python target function to calculate AEP (given `.yaml` turbine locations and farm attributes)

We selected the programming language Python, since it is widely used by researchers in the industry, and is open source. Participants were allowed to alter our specific code implementation or replicate the provided model in another language to speed up the code or for compatibility with their optimization methods. This was with the understanding, however, that final wind farm layouts would be evaluated with the original Python code that we provided.

C. Case Study 4: Discreet Boundary Regions with Concavities

The intent of this case study was to assess both (1) the effects different wake models have on optimization results and (2) how participants addressed a farm with discreet boundary sections seperated by non-viable areas. Like the relationship between cs2 and cs1, cs4 differs from cs3 in that no wake model was provided. Participants were free to choose their preferred EWM and optimization method combination.

The wind farm in cs4 consisted of eighty-one (81) turbines. It was entirely up to participants and their optimizers how to apportion the turbines across the disparate sections of the farm. The wind rose and wind speed frequencies were the same as in cs3.

III. Results

A. Case Study 3: Concave Boundary

B. Case Study 4: Disjoint Boundary

IV. Conclusion

*https://github.com/byuflowlab/iea37-wflo-casestudies/cs2-4/

Acknowledgments

This work was authored [in part] by the National Renewable Energy Laboratory, operated by Alliance for Sustainable Energy, LLC, for the U.S. Department of Energy (DOE) under Contract No. DE-AC36-08GO28308. Funding provided by the U.S. Department of Energy Office of Energy Efficiency and Renewable Energy Wind Energy Technologies Office. The views expressed in the article do not necessarily represent the views of the DOE or the U.S. Government. The U.S. Government retains and the publisher, by accepting the article for publication, acknowledges that the U.S. Government retains a nonexclusive, paid-up, irrevocable, worldwide license to publish or reproduce the published form of this work, or allow others to do so, for U.S. Government purposes.

The authors gratefully acknowledge the following individuals, in alphabetical order, as submitting participants in the case study:

- Tim Camp, Director, Turbine Engineering
- Abhinav Prakash, Ph.D. Student, Texas A&M University
- Erik Quaeghebeur, Dr.ir, Delft University of Technology
- Sebastian, Sanchez Perez Moreno, Ph.D. Student, Delft University of Technology
- Landon Wiley, M.Sc Student, Brigham Young University

Appendix

References

[1] Herbert-Acero, J. F., Probst, O., Réthoré, P.-E., Larsen, G. C., and Castillo-Villar, K. K., "A Review of Methodological Approaches for the Design and Optimization of Wind Farms," *Energies*, 2014, p. 23.

[2] Burton, T., Sharpe, D., Jenkins, N., and Bossanyi., E., *Wind Energy Handbook*, Wiley, 2001.

[3] Larsen, G. C., Aagaard Madsen, H., Larsen, T. J., and Troldborg, N., "Wake Modelling and Simulation," Tech. rep., Technical University of Denmark, 2008.

[4] Sanderse, B., "Aerodynamics of Wind Turbine Wakes," *Energy Resource Center of the Netherlands*, 2009, p. 46.

[5] Larsen, G. C., "A Simple Stationary Semi-Analytical Wake Model," Tech. rep., Technical University of Denmark, 2009.

[6] Vermeer, L., Sorensen, J., and Crespo, A., "Wind Turbine Wake Aerodynamics," *Progress in Aerospace Sciences*, Vol. 39, 2003, pp. 467–510.

[7] Ott, S., Berg, J., and Nielsen, M., "Linearised CFD Models for Wakes," Tech. rep., Technichal University of Denmark, 2011.

[8] Jensen, N., "A Note on Wind Generator Interactions," Tech. rep., Risø National Laboratory, 1983.

[9] Nocedal, J., and Wright, S. J., *Numerical Optimization*, 2nd ed., Springer, 2006.

[10] Kramer, O., Ciaurri, D. E., and Koziel, S., *Comput. Optimization, Methods and Algorithms*, Springer, 2011.

[11] McWilliam, M. K., Zahle, F., and Dykes, K., "IEA Task 37 on System Engineering in Wind Energy The Aerodynamic Only Optimization Case Study," , May 2017.

[12] Agency, N. E., "Borssele Wind Farm Zone Wind Farm Sites III IV Project and Site Description," , August 2016.

[13] Bortolotti, P., Dykes, K., Merz, K., Sethuraman, L., and Zahle, F., "IEA Wind Task 37 on System Engineering in Wind Energy, WP2 - Reference Wind Turbines," Tech. rep., National Renewable Energy Laboratory (NREL), Golden, CO., May 2018.

[14] Bastankhah, M., and Porté-Agel, F., "Experimental and Theoretical Study of Wind Turbine Wakes in Yawed Conditions," *J. Fluid Mech.*, Vol. 806, 2016, pp. 506–541.

[15] Thomas, J. J., and Ning, A., "A Method for Reducing Multi-Modality in the Wind Farm Layout Optimization Problem," *Journal of Physics: Conference Series*, Vol. 1037, The Science of Making Torque from Wind, Milano, Italy, 2018, p. 10.

[16] Niayifar, A., and Porté-Agel, F., "Analytical Modeling of Wind Farms: A New Approach for Power Prediction," *Energies*, 2016.